

# IMPROVED KNOWLEDGE OF CWR TRACK

**Coenraad Esveld**

Professor of Railway Engineering TU Delft  
Project Manager of ERRI Committee D202  
Email: c.esveld@ct.tudelft.nl

## **ABSTRACT**

In 1992 the International Union of Railways (UIC) commissioned a study from ERRI entitled "Improved knowledge of CWR, including switches" and the work was assigned to the ERRI D 202 Specialists' Committee. There were basically four parts to the work: a. Development of theoretical models, b. Experimental work to determine input values for the models and to validate the models, c. Revision of UIC leaflets on CWR and d. Non-destructive measurement of longitudinal rail forces due to temperature. Three models were developed: CWERRI, which analyses track stability in combination with longitudinal and vertical loads, including dynamic effects and yielding of ballast under combined load situations; LONGIN, which permits analysis of creep phenomena under longitudinal train loads and also models curve breathing; and TURN, a program which allows analysis of turnouts in combination with the finite element package ALGOR. The models were developed at TU Delft, The Netherlands and TU Kraków, Poland.

The experimental work was primarily focused on obtaining lateral track resistance data. One of the objectives was to link the European data to test data from single-tie experiments in North America. Fundamental aspects of three-dimensional ballast yield were also investigated.

## **1. INTRODUCTION TO THE WORK OF D202**

In October 1991 the ORE S 1061 feasibility study, with the title 'Improved knowledge of forces in CWR track (including switches), was officially approved by the Control Committee. The main objective of the work proposed was intended to result in a uniform safety philosophy for CWR track, guidelines and recommendations concerning its laying, maintenance and diagnosis, and to serve as a basis for updating and clarifying Leaflet 720 R. The work was setup in 1992 with emphasis to the development of theoretical models, and in-situ verification tests, supplemented with laboratory tests. Priority was given to:

- Models to describe the behaviour of long bridges, switches, tight curves, both from the aspect of longitudinal forces and lateral stability, also taking into consideration dynamics and rheological behaviour;
- Systematic check on stresses in the track;
- Safety rules/criteria/margins, unified methods;
- Influence of parameters like gauge, cant deficiency, axle load, track components and track quality;

## **2. CWERRI**

The CWERRI program was developed by TU Delft in The Netherlands and contained functionality with respect to Lateral and vertical stability of curved track and longitudinal, lateral and vertical forces. The program is able to model multi span bridges with parallel tracks loaded by train set. The basic features of the model are as follows:

- Three-dimensional modeling and calculation tool
- Longitudinal, lateral and vertical forces
- Lateral and vertical track stability
- Thermal and mechanical loads
- Complete train loads, taking uplift waves into account
- Three-dimensional ballast yield, taking the influence of vertical loads into account
- Track/bridge interaction, including the effects of end rotation
- Multi-span bridges with parallel tracks

This section briefly describes some examples of calculations consisting of a buckling sensitivity analysis on curved CWR track, followed by a sensitivity analysis. The longitudinal force problem is illustrated by a fly-over study based on input data from Netherlands Railways.

In order to have a good overview of the theory on CWR track it was decided to write a state of the art report in which the present development of the theory would be summarized. This work was subcontracted by Dr. Gopal Samavedam of Foster-Miller, USA and resulted in publication [3].

## 2.1 BUCKLING ANALYSIS OF CURVED CWR TRACK

Using the CWERRI model, a sensitivity analysis was carried out on the track structure of Fig. 1, by varying such parameters as the half wavelength of the misalignment, the curve radius, the peak and limit resistance of the lateral ballast strength and the torsional stiffness of the fastening system [19]. The dimensions and properties were chosen in accordance with results published by Kish [18]. The track model was 47.5 m long, with a horizontal curve radius of 400 m. A longitudinal spring was added at the boundaries, in order to model the longitudinal behavior of linear elastic tangent track up to infinity. The misalignment in the middle was characterized by a half sine wave with a length of 9.144 m (360 in.) and an amplitude of 0.0381 m (1.5 in.). The track component properties were as follows: rails: AREA#136, sleeper spacing: 0.61 m and vertical ballast stiffness: 68 900 kN/m per meter track. The constitutive behavior of the ballast spring is given in Fig. 2 and the values for  $F_p$  and  $F_l$  in the absence of vehicle load are given in Tab. 1.

The track was loaded vertically by a hopper car with two bogies, represented by four vertical axle loads of 293 kN each, as indicated in Fig. 3.

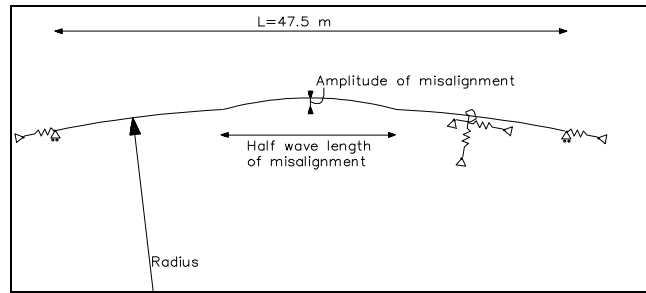


Fig. 1: Top view of track model

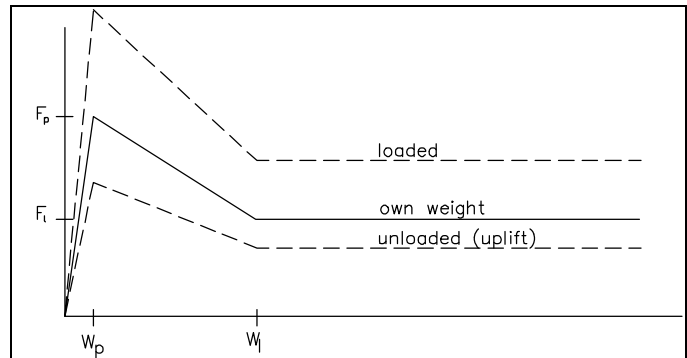


Fig. 2: Model of lateral ballast behavior for different vertical loadings

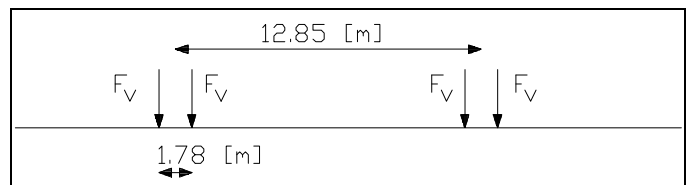


Fig. 3: Vertical load applied on track model ( $F_v = 293$  kN)

The track was loaded by increasing the temperature from 0°C to 100°C. Fig. 4 shows lateral deformation in the center of the model against temperature increase. In [4] these results were compared with the values produced by the model described in [18], which was validated by a number of full-scale track buckling tests carried out in the USA, both with and without moving trains. The values produced by both models are very close. The plot in Fig. 4 is characterized by two points. The first point is the temperature  $T_{b,max}$  (49.4°C), at which buckling starts, and which is the highest point in the figure. After this point, the temperature drops and deformations grow rapidly. The second point is the minimum temperature  $T_{b,min}$  (33.5°C) that occurs after buckling has started. From a safety point of view this is the most important value.

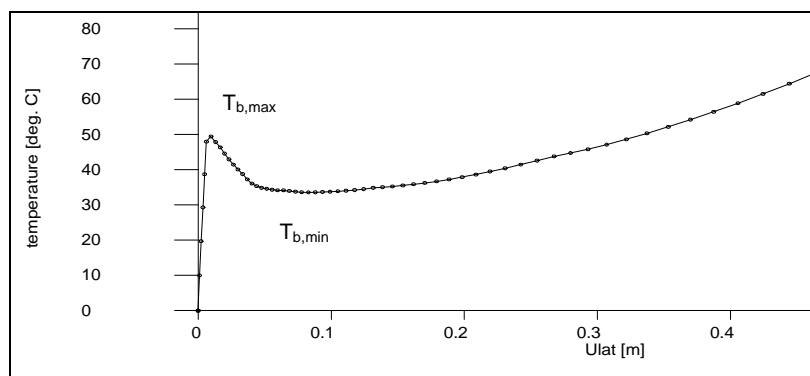


Fig. 4: Lateral deformation in the middle of the model

## 2.2 Sensitivity analysis

The next part of this paper discusses the sensitivity of  $T_{b,max}$ <sup>1</sup> and  $T_{b,min}$  to the parameter variations shown in Tab. 1. Each parameter was varied over a practical range while keeping all other parameters constant at the “fixed value”.

Fig. 5 shows the calculated results for  $T_{b,max}$  and  $T_{b,min}$  as a function of curve radius. The yield force is affected by the vertical track load. The reference value for the radius is 400 m. Buckling starts at lower temperatures in small-radius curves.

Parameter	Fixed value	Range
Radius [m]	400	100 - Tangent
Lateral peak resistance ( $F_p$ ) [N per m track]	17 508	8 754 - 26 262
Lateral limit resistance ( $F_l$ ) [N per m track]	9 630	4 815 - 14 445
Longitudinal stiffness [N/m per m track]	1.378e6	1.0e5 - 1.0e7
Torsional stiffness [Nm/rad per m track]	1.1125e5	0.0 - 3.0e5
Amplitude of misalignment [m]	0.0381	0.008 - 0.05
Half wavelength of misalignment [m]	4.572	1.2 - 9.6

Tab. 1: Parameters in sensitivity study

The ballast behavior, represented by the lateral peak and limit resistance, was varied over a range of 50% to 150% of the reference value and Fig. 6 shows  $T_{b,max}$  to be more sensitive to this factor. Fig. 7 indicates that varying the longitudinal ballast stiffness has little influence on  $T_{b,max}$ . The torsional stiffness, often associated with the frame stiffness of the track, influences neither  $T_{b,max}$  nor  $T_{b,min}$ , as can be seen from Fig. 8.

From Fig. 9, it is apparent that the amplitude of the misalignment has a marked influence on  $T_{b,max}$ , whereas  $T_{b,min}$  is less affected. The half wavelength, shown in Fig. 10, is related to the amplitude of the misalignment. In the calculations, a fixed relationship was assumed, based on statistical analysis of measurement data.

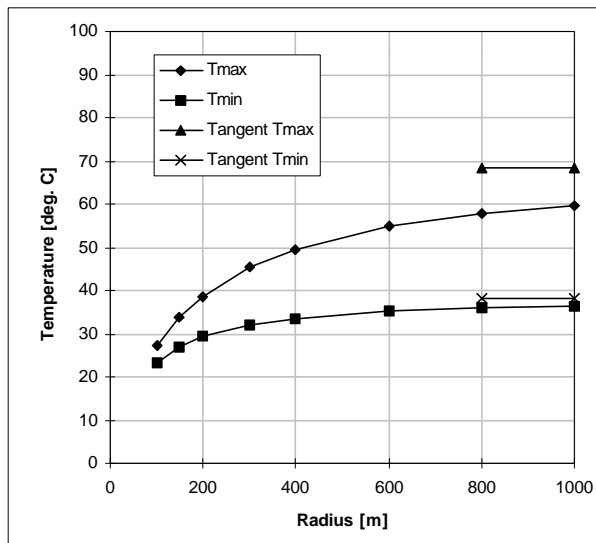


Fig. 5: Influence of radius

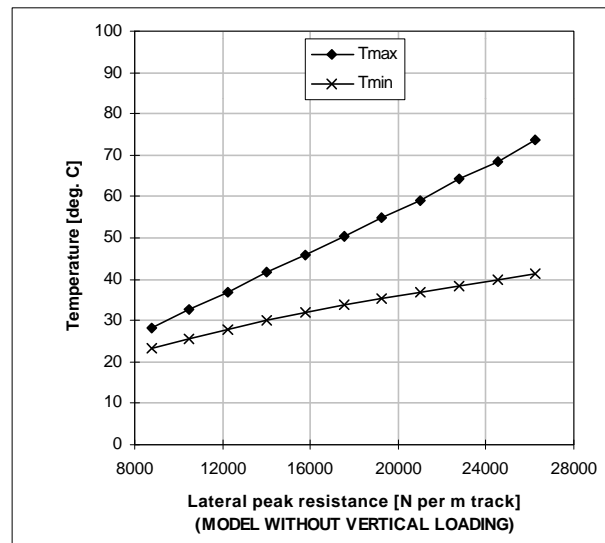


Fig. 6: Influence of lateral peak resistance

<sup>1</sup>  $T_{b,max}$  and  $T_{b,min}$  are referred to in some of the figures as  $T_{max}$  and  $T_{min}$

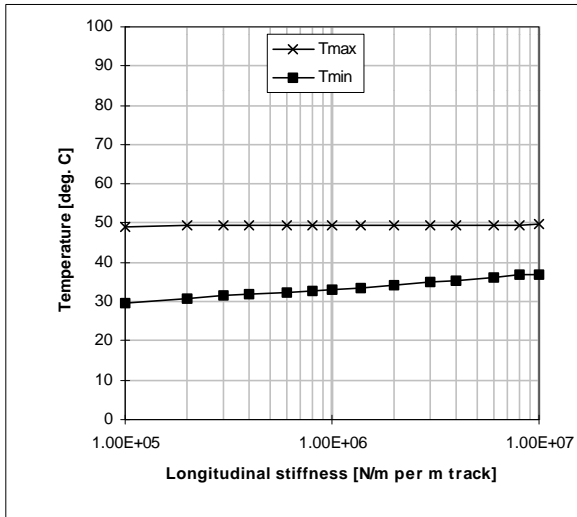


Fig. 7: Influence of longitudinal stiffness

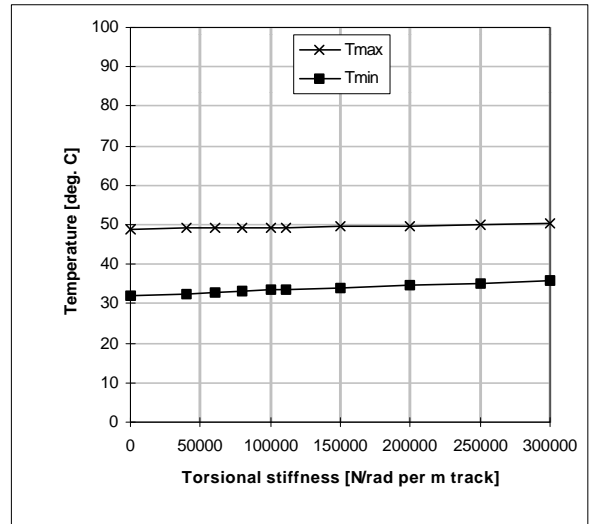


Fig. 8: Influence of torsional stiffness

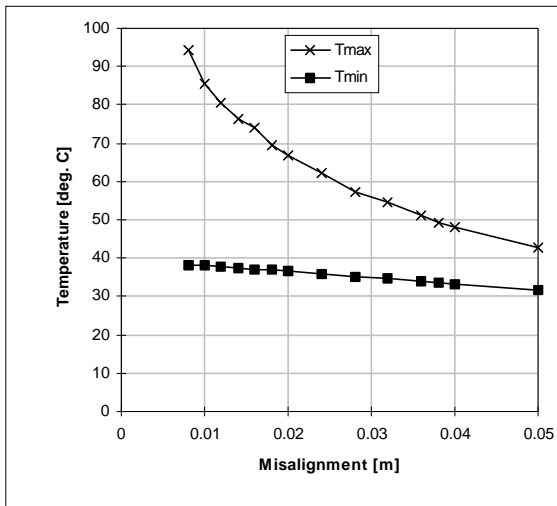


Fig. 9: Influence of misalignment

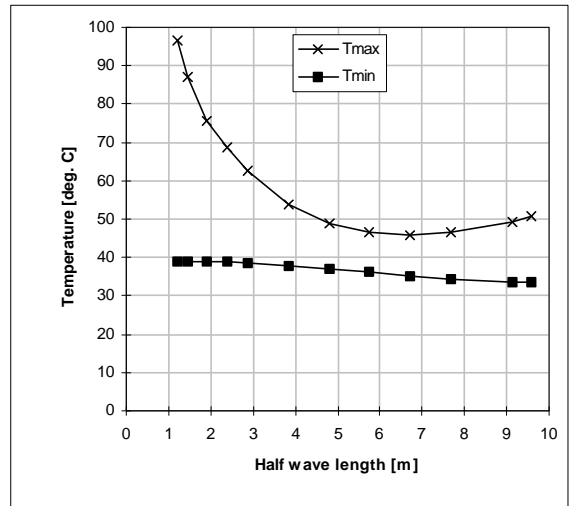


Fig. 10: Influence of half wavelength

### 2.3 Safety analysis

A major application of CWERRI is its use as a tool for safety analyses. Together with the DOT's CWR-BUCKLE program, a large number of calculations has been performed in developing safety criteria to be implemented in the new edition of UIC Leaflet 720.

The results of the calculations with CWERRI [4] are expressed in terms of the temperature of the rail above the normal or neutral temperature. Normally, there is an area between two limits ( $T_{b,min}$  and  $T_{b,max}$ ) wherein buckling may occur.

It is widely assumed that track buckling in this area between  $T_{b,min}$  and  $T_{b,max}$  depends on the external addition of energy to the buckled track, e.g. by a moving train. For temperatures close to  $T_{b,min}$  the amount of energy is much larger than close to  $T_{b,max}$ . This amount can be calculated by a program called CWR-Buckle which was developed in the USA [18] for the same purpose as CWERRI: track safety against buckling.

The parametric studies on track buckling [9] were carried out for the following structures:

1	High speed track	tangent	concrete sleepers
2	Main line track	radius 900 m	concrete sleepers
3	Main line track	radius 900 m	wooden sleepers
4	Secondary line track	radius 600 m	concrete sleeper
5	Secondary line track	radius 600 m	wooden sleepers
6	Freight line track	radius 300 m	concrete sleeper
7	Freight line track	radius 300 m	wooden sleepers

Each structure was analyzed for three different misalignments with lengths of 8 m, 10 m and 12 m. The magnitudes (twice the amplitude) were:

Structure 1: total misalignments: 8/12/16 mm  
 Structures 2 and 3: total misalignments: 10/14/18 mm  
 Structures 4 and 5: total misalignments: 14/18/22 mm  
 Structures 6 and 7: total misalignments: 14/22/30 mm

For each misalignment, the quality of the ballast material (expressed in  $F_p$  (peak) and  $F_l$  (limit) values) was altered three times: low, average and high quality. The parametric values were expressed in terms of the force required to move a 1-metre track panel laterally through the ballast over a predefined number of millimeters ( $w_p$ : 2 mm or 5 mm).

Concrete sleepers: 10/10, 15/12 and 20/16 kN/m'  
 Wooden sleepers: 7/7, 10/10 and 15/12 kN/m'

In addition, the influence of the rail fastening system in the lateral direction was altered twice: a small, rigid fixture resisting torsion can be taken into account as  $k_t$  in terms of the required moment per radian per meter track. Again, the values depend on the sleeper type.

Concrete sleepers: 75 and 150 kNm/rad/m'  
 Wooden sleepers: 150 and 250 kNm/rad/m'

The parametric values for the friction coefficient for lateral resistance between ballast and sleeper were:

Concrete sleepers:  $\phi = 0.86$   
 Wooden sleepers:  $\phi = 1.2$

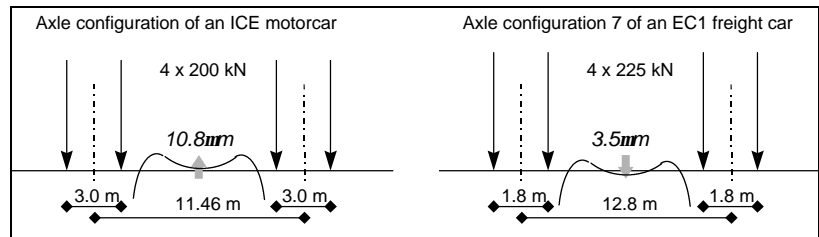


Figure 11: Axle configurations for passenger and freight vehicles

The vertical track stiffness values  $k_v$ , expressed per meter of track, were:

Structures 1, 2 and 3: 100 MN/m/m'  
 Structures 4, 5, 6 and 7: 70 MN/m/m'

For the seven structures, two different vehicles were chosen (Figure 11). The most severe cases of track buckling occur if the axle configuration of the vehicle leads to significant lifting of the track according to the (static) deflection curve. The following combinations of vehicle and structure were chosen:

Structures 1, 2 and 3: ICE power car  
 Structures 4, 5, 6 and 7: EC 1 vehicle axle configuration 7 for wagons

In total, 252 calculations were carried out.

The basic results of the analysis are comprised of  $T_{b,max}$  and  $T_{b,min}$ , explained in Figure 12.

The left graph shows the situation found in almost 90% of cases. The full graph comprises two branches: a linear elastic deformation line starting at the origin and a plastic irreversible deformation line with a minimum value called  $T_{b,min}$ . Normally  $T_{b,max}$  is found at the intersection of both branches.

The right-hand graph depicts the behaviour in the other 10% of cases. This behaviour is mainly connected with and caused by excessively low lateral resistance, i.e. low ballast quality. If elastic deformation has reached its maximum below the minimum of the plastic deformation branch “progressive buckling” (PB) occurs.

### Safety limits

For track safety,  $T_{allow}$  is the maximum allowable temperature above the neutral temperature of the rail that is considered safe as far as track buckling is concerned.  $T_{allow}$  can be seen as a buffer with regard to many phenomena that increase rail temperature or an equivalent axial compressive stress in the rail, pushing it into the dangerous “buckling” range. These phenomena are:

- Air temperature
- Sunlight
- Eddy current brakes
- Interaction with other structures, such as bridges

The first and second items generally take up about 30°C to 40°C of the available temperature buffer, depending on local circumstances. This means that specific structures with a  $T_{allow}$  value lower than 40°C will certainly encounter

buckling problems in summer or under other high-temperature conditions. With  $T_{allow}$  above 40°C, structures can be exposed to eddy current brakes or to external forces from other structures, as long as the equivalent temperature increase remains within the calculated buffer of degrees.

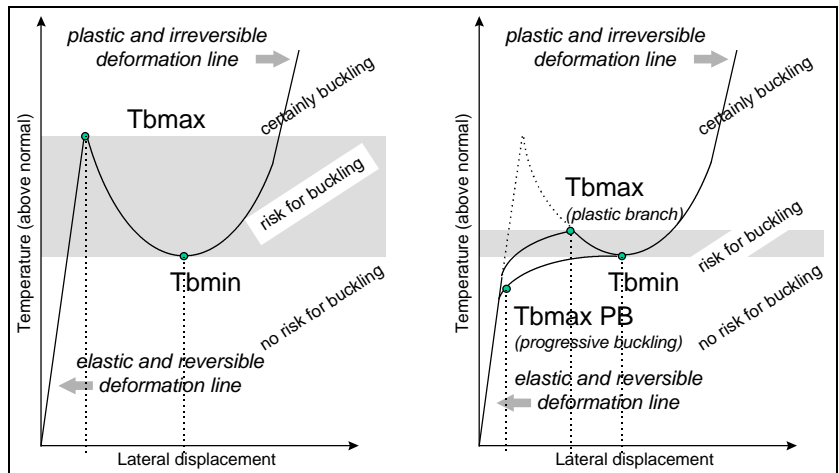


Figure 12: Temperature vs. lateral displacement for good ballast (left) and poor ballast (right)

For the structures discussed previously, the safety margins in terms of  $T_{allow}$  were determined as follows:

CWERRI	$T_{allow} = T_{b,min} + 0.25 (T_{b,max} - T_{b,min})$
CWR-Buckle	$T_{allow}$ is the temperature at which the energy required to buckle the track structure is 50% of the energy required to buckle the track structure at $T_{b,min}$ , which is equivalent to: $T_{allow} = T_{b,min} + 0.25 (T_{b,max} - T_{b,min})$

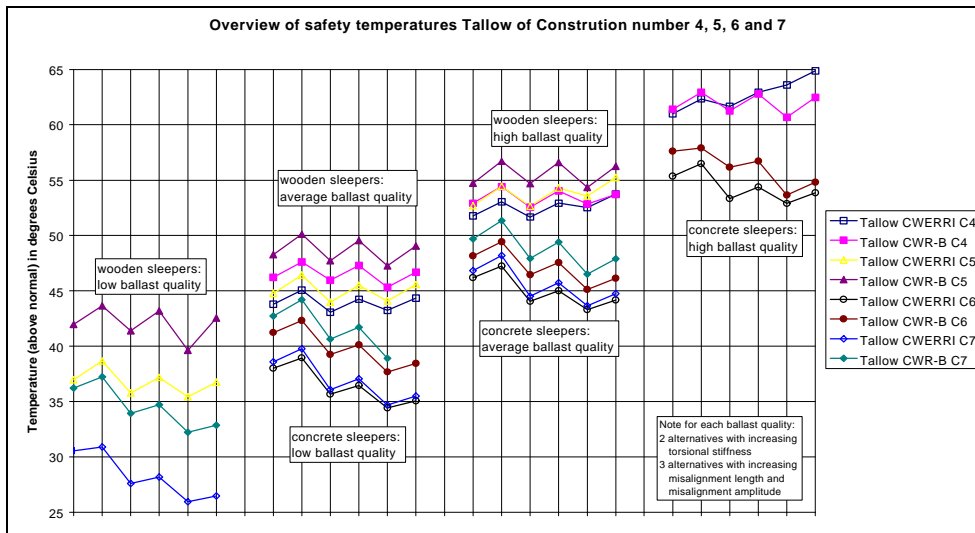


Figure 13: Overview of freight track safety temperatures

Figures 13 and 14 show the results of the calculations in Cases 2 and 3, for passenger and freight track. It is remarkable that the differences in the results for similar structures with small, moderate and large misalignments are quite small (range < 5°C) while the differences for low, average and high ballast quality are almost constant ( 8.5°C - 10°C for CWERRI results, 6°C - 9°C for CWR-Buckle results). These differences between two ballast qualities are larger than the differences between  $T_{b,min}$  values for two ballast qualities described in Case 1. It can be concluded that the values of  $T_{b,max}$  and energy for specific structures increase (more than linearly) if  $T_{b,min}$  increases. The differences in the results for concrete and wooden sleepers are almost negligible.

Figures 13 and 14 reveal that there is a difference of approximately 10°C between low, average and high quality.

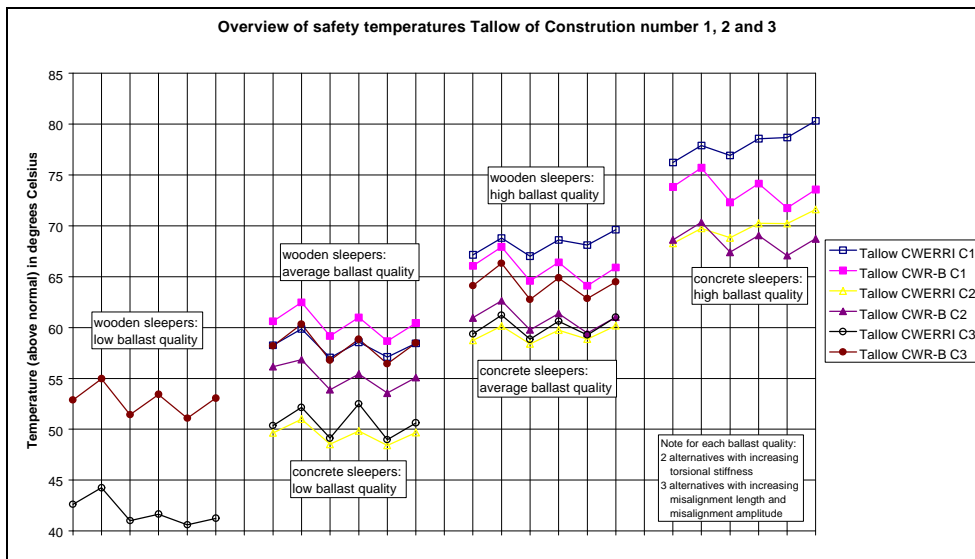


Figure 14: Overview of passenger track safety temperatures

On the basis of this large number of calculations, the ERRI D 202 Specialists' Committee proposed the following safety criteria:

- If  $\Delta > 20 \text{ }^\circ\text{C}$ :  $T_{allow} = T_{b,min} + 25\% \text{ of } \Delta$
  - If  $5 \text{ }^\circ\text{C} < \Delta < 20 \text{ }^\circ\text{C}$ :  $T_{allow} = T_{b,min}$
  - If  $0 \text{ }^\circ\text{C} < \Delta < 5 \text{ }^\circ\text{C}$ :  $T_{allow} = T_{b,min} - 5 \text{ }^\circ\text{C}$
  - If  $\Delta < 0 \text{ }^\circ\text{C}$ : not allowable in main lines.
- With  $\Delta = T_{b,max} - T_{b,min}$

## 2.4 LONGITUDINAL FORCES IN THE MAARTENSDIJK FLY-OVER

Figs 15 to 17 show how CWERRI was used to model a fly-over built for Netherlands Railways. The longitudinal ballast springs between rail and bridge were modeled as indicated in Fig. 12, and were connected in the middle of the tie and on top of the bridge deck.

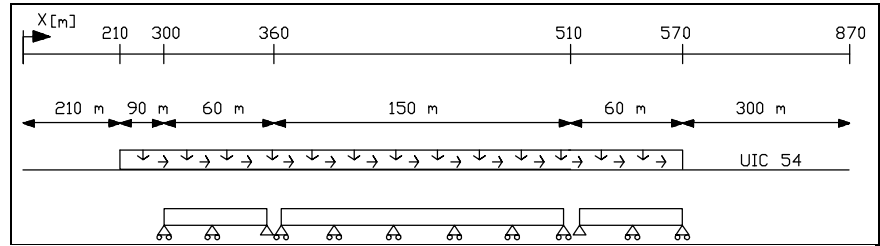


Fig. 15: Track model

The model was loaded in four steps: a thermal load consisting of a temperature increase of 40°C for the rails and 20°C for the bridge, 20 cars loading the track with 80 axles, according to Figs 15 and 17, each axle generating 225 kN vertically and 45 kN longitudinally. The longitudinal ballast strength was 20 kN per running meter track unloaded and 50 kN loaded. In the third load step the track was unloaded from the longitudinal and vertical axle loads. Finally rail and bridge were thermally unloaded, which resulted in residual deformations and forces due to yielding of the ballast.

### Results

Some results are presented here by way of an example, to illustrate the potential of the program. Fig. 18 shows the longitudinal forces in the rails. The relative longitudinal displacements between rails and bridge, an important measure of ballast degradation, are shown in Fig. 19. Obviously, the thermal load step results in an asymmetric response, because both construction and load are asymmetric. Unloading in the fourth load step results in residual forces and displacements. The largest residual values in rail and ballast are obtained at both ends of each of the three bridge spans, where most of the ballast yield took place.

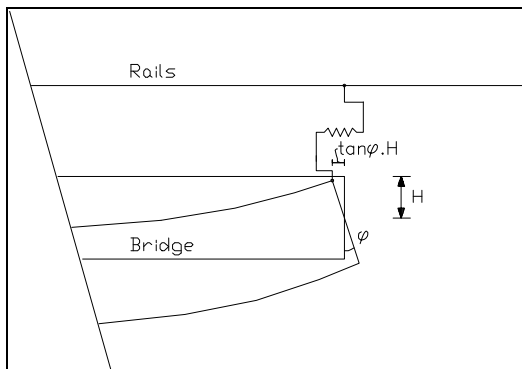


Fig. 16: Eccentricity of top and center of deck

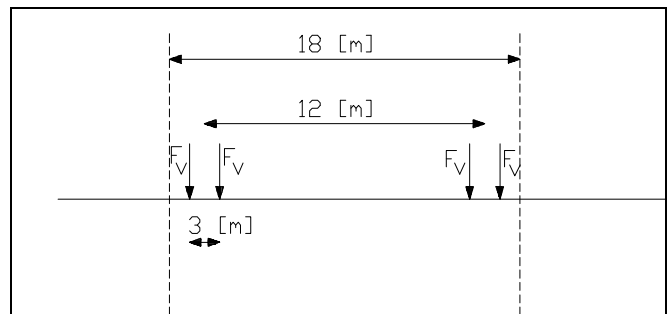


Fig. 17: Loading

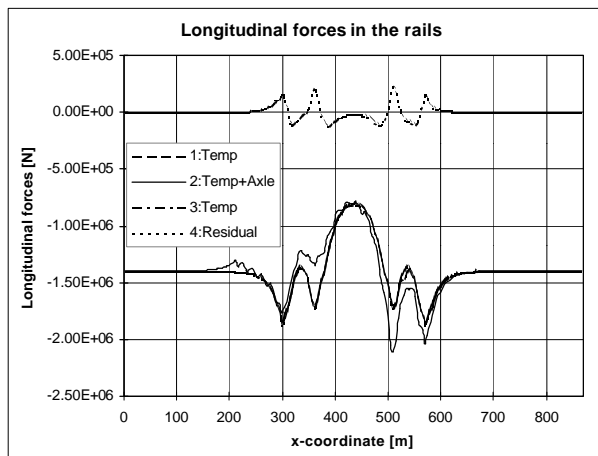


Fig. 18: Longitudinal forces in the rail

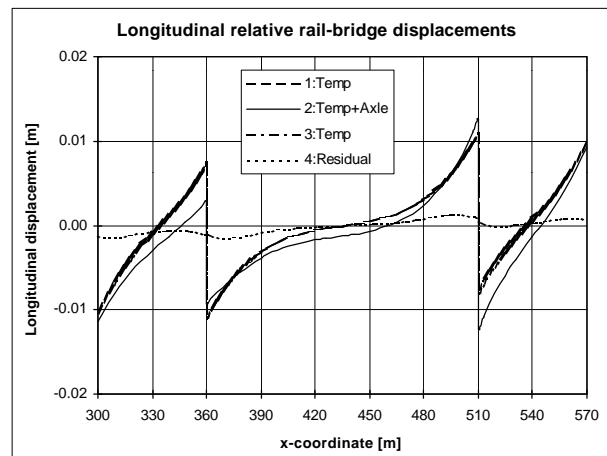


Fig. 19: Relative rail/bridge displacement

## 2.5 LONGIN

The program LONGIN was developed by TU Krakow in Poland with the main emphasis to longitudinal track creep and the behaviour of tight curves. Also the influence of track tamping and ballast cleaning can be simulated.

The scope of the model is outlined in Fig. 20. The load is considered as a quasi-static moving load. The effect of the change in longitudinal resistance under vertical load is included. Ballast and fastener resistance are modeled bi-linearly, as indicated in Fig. 20. Further, it is assumed that the ballast deteriorates with the number of brake applications according to a decaying exponential function of the form:

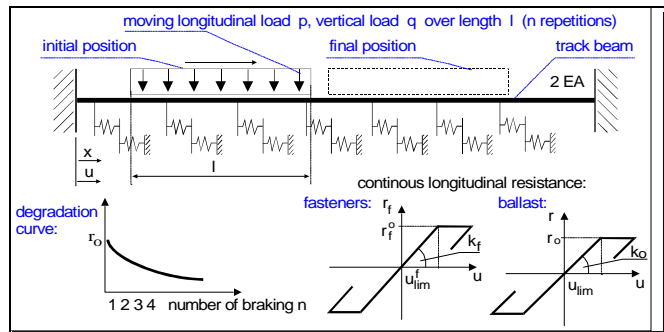


Fig. 20: Creep model

$$r^* = r_0 1.0306 e^{-0.03n}$$

where:  $r_0$  = yield point of the ballast without degradation and  $n$  = the number of loading passes. The sensitivity to ballast and fastener characteristics was investigated in [5]. The parameters were varied around the following mean values:

$r_f^0 = 8.0$  kN/m,  $k_f = 5700$  kN/m/m for the fasteners and  $r_0 = 12.0$  kN/m,  $k_0 = 8000$  kN/m/m for the ballast.

The type of load was chosen in accordance with the data published in [1], i.e. vertical  $q = 86.25$  kN/m; length of the load  $l = 640$  m (DB, heavy); intensity of braking:  $\eta = 0.2$ ;

Longitudinal load is  $p = \eta q$  [kN/m]. Three gradients were considered: 5‰, 10‰ and 15‰. The influence of each gradient was taken into account as an increase in the braking force by the product of the value of the gradient and the braking load. In addition, fixed points were introduced, to model a turnout with a length of 33 m and a longitudinal stiffness of 100 MN/m/m. The turnout was located 10 m ahead of the point where the train stopped.

Fig. 21 summarizes the residual forces versus the number of brake applications. The influence of the gradient is quite significant, as is the effect of ballast degradation.

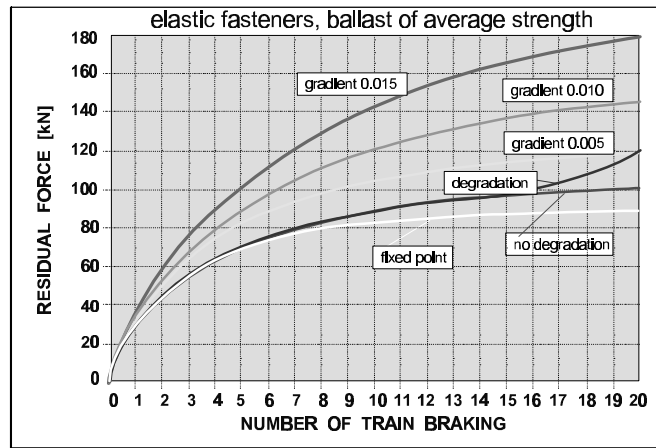


Fig. 21: Examples of creep calculations

### 2.5.1 SHARP CURVES

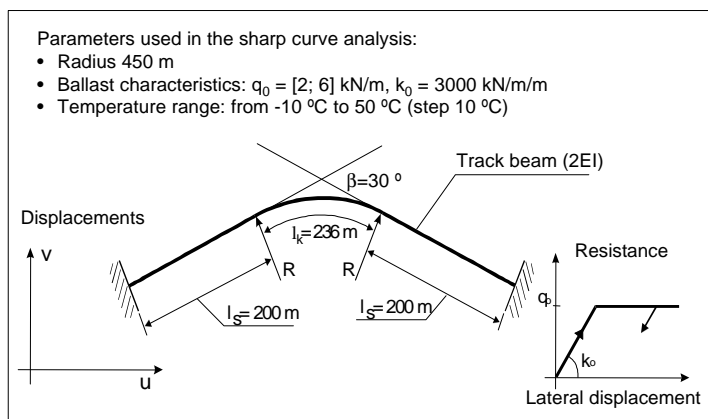


Fig. 22: Model applied for creep in sharp curves

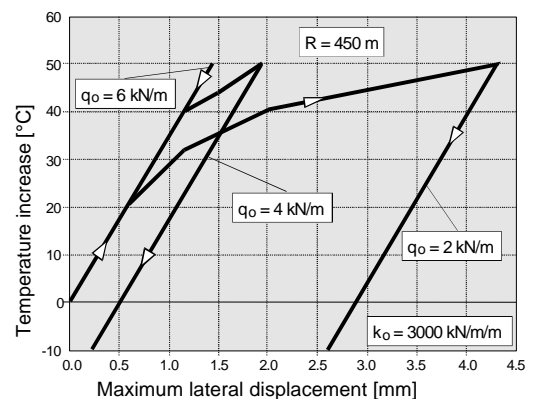


Fig. 23: Lateral movement of sharp curve

The LONGIN model also allows analysis of the lateral breathing of curves. As an example, the curve of Fig. 22, (radius 450 m), was studied with different values of ballast resistance. The results are presented in Fig. 23 and show how important a role ballast properties play.

### 3. TURNOUT ANALYSIS

#### 3.1 Introductory remarks

The TURN program was developed by TU Krakow in Poland for analyzing pre-buckling track problems. The program deals with two dimensional problems and only thermal loads may be considered.

The basic calculation kernel of the TURN program consists of the ALGOR-FEM system for analysis of mechanically nonlinear thermal problems. The TURN program can analyze the following track situations:

- a) simple divergence of track (one turnout) also with circular arc and parallel track,
- b) connection of two parallel tracks by two or four turnouts.

Analysis of other cases is possible but only by use of the original ALGOR system with a less user friendly interface from the point of view of track structure and geometry.

#### 3.2 Description of the modelling in TURN

The physical model of the turnout and adjoining zones may be described as follows:

- stress plane is considered - all elements of the system are treated as two dimensional bodies with constant response parameters in vertical direction;
- only the rails are subjected to uniform temperature increase/decrease; loading, unloading and full cycle of thermal load may be considered;
- all rails and sleepers in the turnout and in adjacent tracks are modeled as perfectly elastic bodies, characterized by Young module  $E_i$ , Poisson coefficients  $\nu_i$  and thermal expansion coefficient  $\alpha$  for rail steel - only frog elements are modeled as non-prismatic body; other elements have constant cross section and switch blades over the not fixed zones are neglected;
- fasteners and ballast are included as substitute quadrangle elements with elastic plastic properties, described by Young module  $E_i$ , Poisson coefficients  $\nu_i$ , yield stresses  $\tau_i$  and tangential module  $T_i$ .

Fig. 24 shows typical system of the elements used in the model.

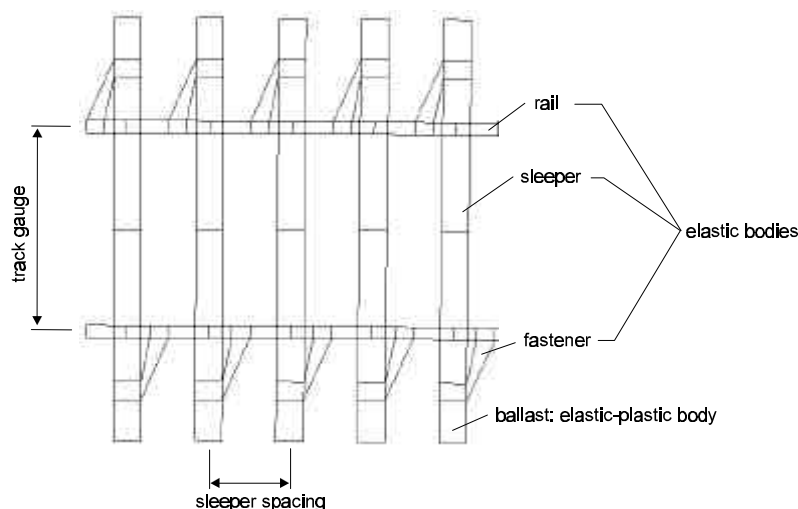


Fig. 24 Physical model of the turnout and adjoining zones - system of the elements

# TURNOUT - v.01

version with ALGOR

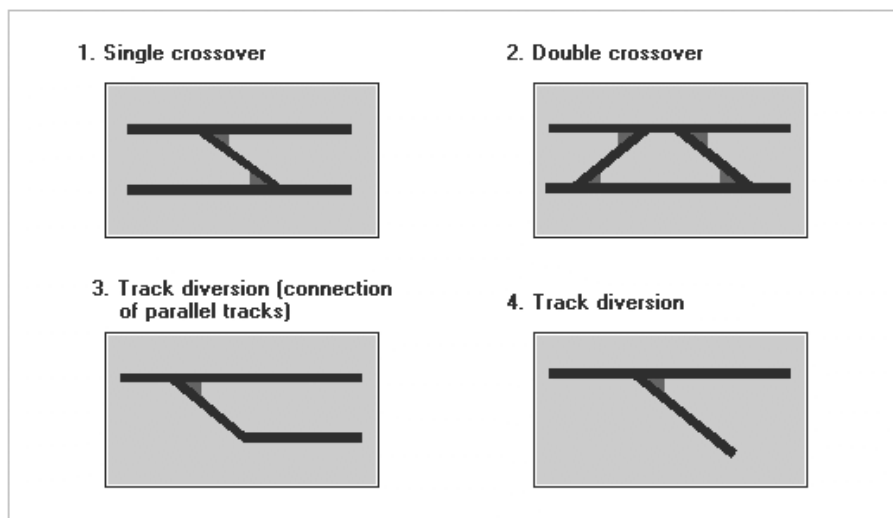


Fig. 25 Track situations possible to analysis with TURN

Rail and sleeper dimensions are real, whereas fasteners and ballast dimension are calculated based on empirical data. The following track situations may be analyzed (see Fig. 25.):

- track diversion
- track diversion (connection of parallel tracks)
- single crossover
- double crossover

The geometry of the entire system and the various types of the turnouts as well as track structure parameters are input via a user friendly interface. Stresses and displacements are calculated using the original ALGOR procedures. The stresses in the rails are then recalculated and the longitudinal forces and displacements are stored to obtain user friendly output.

### 3.3 Comparison with empirical data

The model was tested for:

- \* determination of the length of the adjoining zones for obtain correct solution in the turnout zone;
- \* determination of numerical parameters (necessary step of loading and number of iterations);
- \* comparison of numerical results with empirical data.

Basic tests were carried out for the track situation, presented in Fig 26, i.e. the following parameters:

- \* type of the track structure in turnout and adjacent zones: UIC-60 rails, wooden sleepers with a length of 2.5 m, sleeper spacing 0.6 m and cross section 0.26 x 0.16 m, rigid fasteners and elastic ballast properties : 3000 kN/m per sleeper in longitudinal direction and 2000 kN/m per sleeper in lateral direction;
- \* type of turnout: angle 1:9, radius of curvature 300 m;
- \* length of the turnout and adjacent zone  $L = 100 - 450$  m,
- \* situation parameters: parallel tracks distance - 4.5 m, radius of curvature of diverging track - 300 m;
- \* loading - uniform temperature increase of all rails: 50 °C.

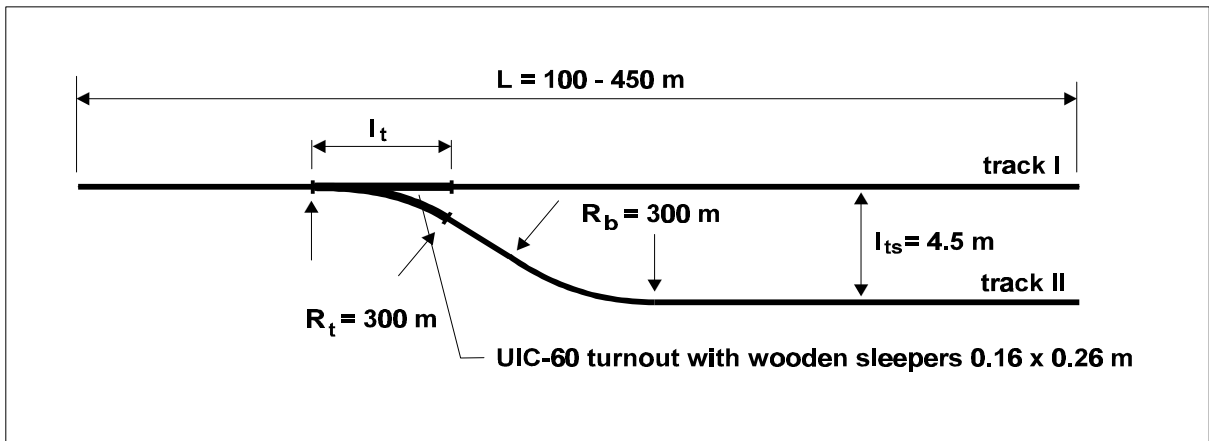


Fig. 26 Diagram of the turnout and adjacent zones used for numerical tests and calculations with the TURN program

Fig. 27. shows an example of the effect of the total length of the system  $L$  on the maximum lateral displacements  $v_{max}$ . As can be seen from the graph, in order to obtain a stable solution the length of the adjoining zones need to be about 250 m either side of the system considered.

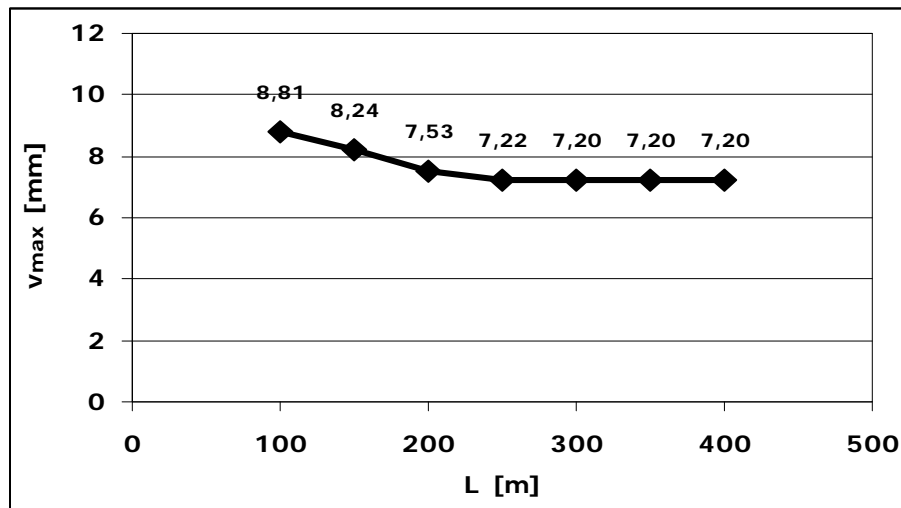


Fig. 27 Effect of the total length of the system  $L$  on the maximum lateral displacements

Fig. 28. presents a numerical and an empirical distribution of the relative longitudinal force in the external rail of the system. The empirical data was originally from France. The coefficient  $N/N_c$  shows the longitudinal force in the external rail of the straight track of the turnout in relation to the thermal force  $N_c = \sigma * E * \Delta T * A_r$ , where:

- $\sigma$  – thermal expansion coefficient [ $1/^\circ\text{C}$ ],
- $E$  – Young's modulus [ $\text{kN}/\text{m}^2$ ],
- $A_r$  - rail cross section [ $\text{m}^2$ ],
- $\Delta T$  – temperature increase [ $^\circ\text{C}$ ]

As can be seen, the empirical and numerical data are similar. Other numerical tests, also for non-linear problems, have shown that a solution is impossible for very weak ballast. However, convergence is obtained with typical ballast (even though it may be weak). Between 3 and 8 loading steps are required according to the type of problem for a simple case (loading applies once). Approximately 15 iterations will be required. The necessary calculation time and computer memory depend on the type of track situation considered.



Fig. 28 Comparison between numerical and empirical results.

### 3.4 Welded group of turnouts

Consider the track layout shown in Fig. 29.

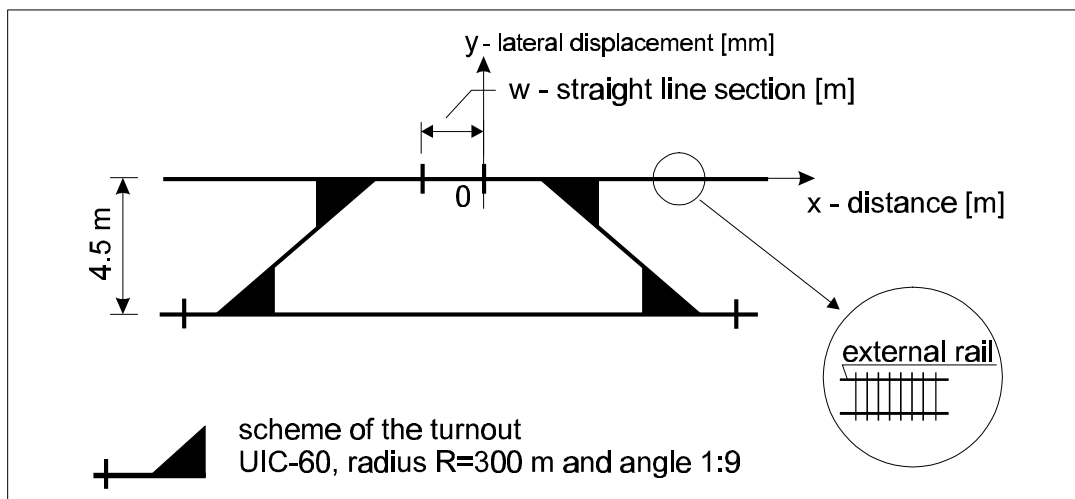


Fig. 29 Track layout used in the analysis

When the TURN program is used with the track model shown in Fig. 30, the results summarized in Fig. 31 - 33 are obtained.

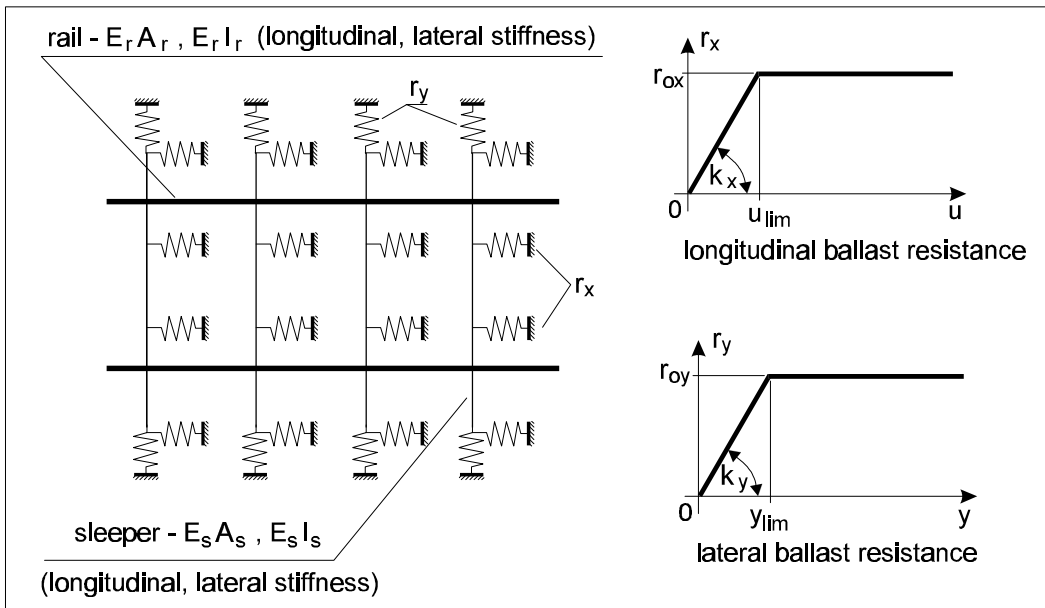


Fig. 30 2-D model of track structure

All calculations have been carried out for a uniform thermal load  $DT = 50^\circ C$  and equivalent ballast resistances (per one meter of track):

- a) longitudinal direction  $k_x = 5000 \frac{kN}{m^2}, r_{ox} = 18 \frac{kN}{m},$
- b) lateral direction  $k_y = 5000 \frac{kN}{m^2}, r_{oy} = 12 \frac{kN}{m}.$

Fig. 31 shows the distribution of lateral displacement and Fig. 32 shows the distribution of longitudinal force in the external rail for the straight track section with the distance between turnouts being  $w = 0, 10, 20$  and  $50$  m (minus sign denotes compression force).

Fig. 33 shows the effect of the length of the straight track  $w$  on the maximum lateral displacement of the external rail of the track. From the calculations it follows that the length of the straight track section between turnouts 1 and 2 has a significant influence on the force and displacement state of the system under thermal load - in the case analyzed, if  $w = 10$ , the maximum lateral displacement (i.e. 50% of the  $u_{lim} = 4$  mm) and maximum longitudinal force occur. With a section length  $w = 50$  m, practically the same displacement and force distribution occur as with  $w = 20$  m.

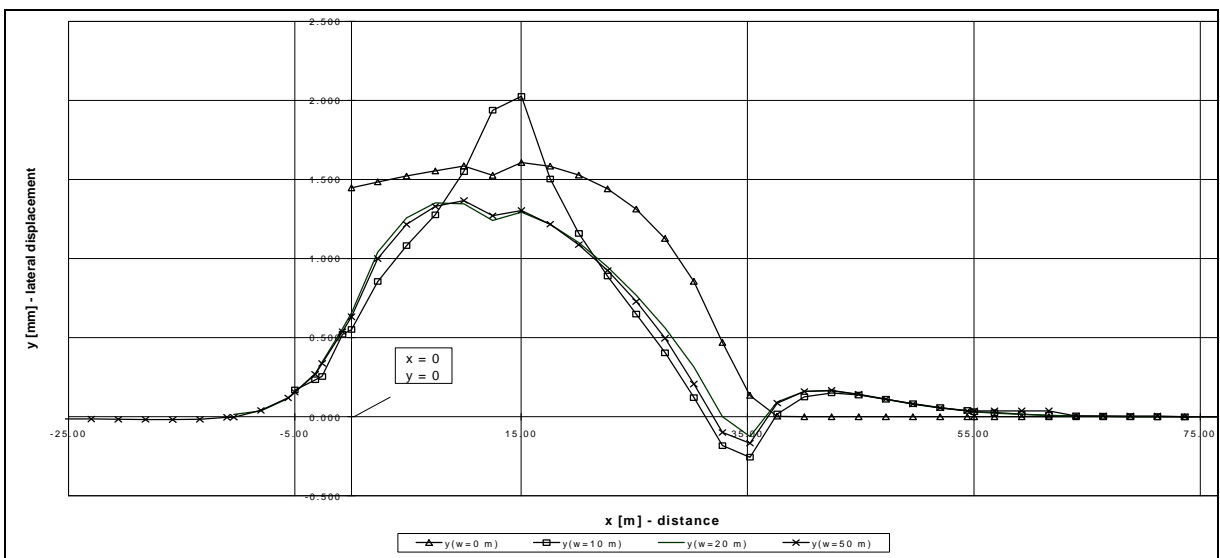


Figure 31: Distribution of lateral displacements in external rail

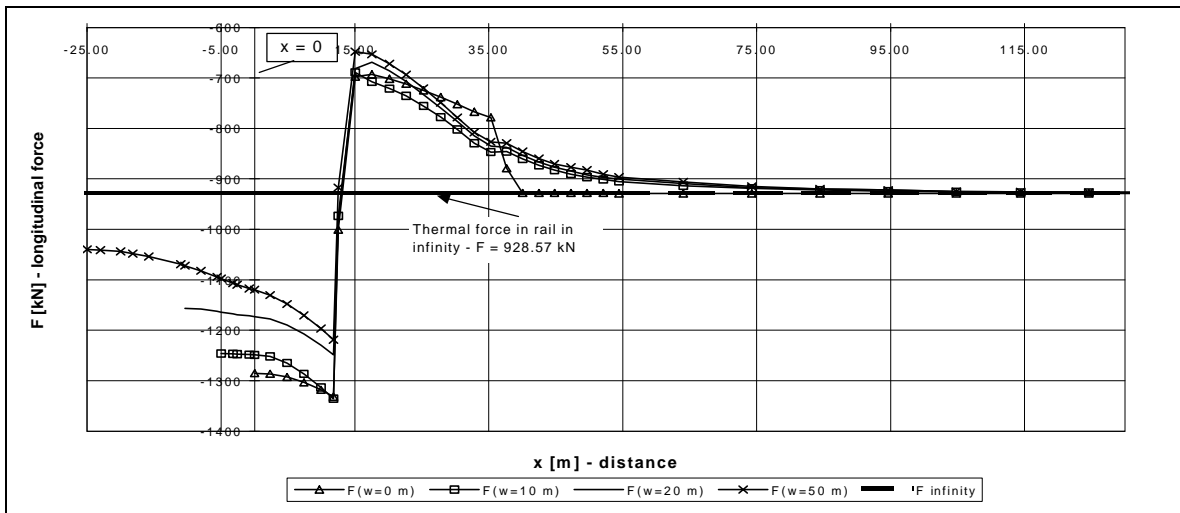


Figure 32: Distribution of longitudinal forces in external rail

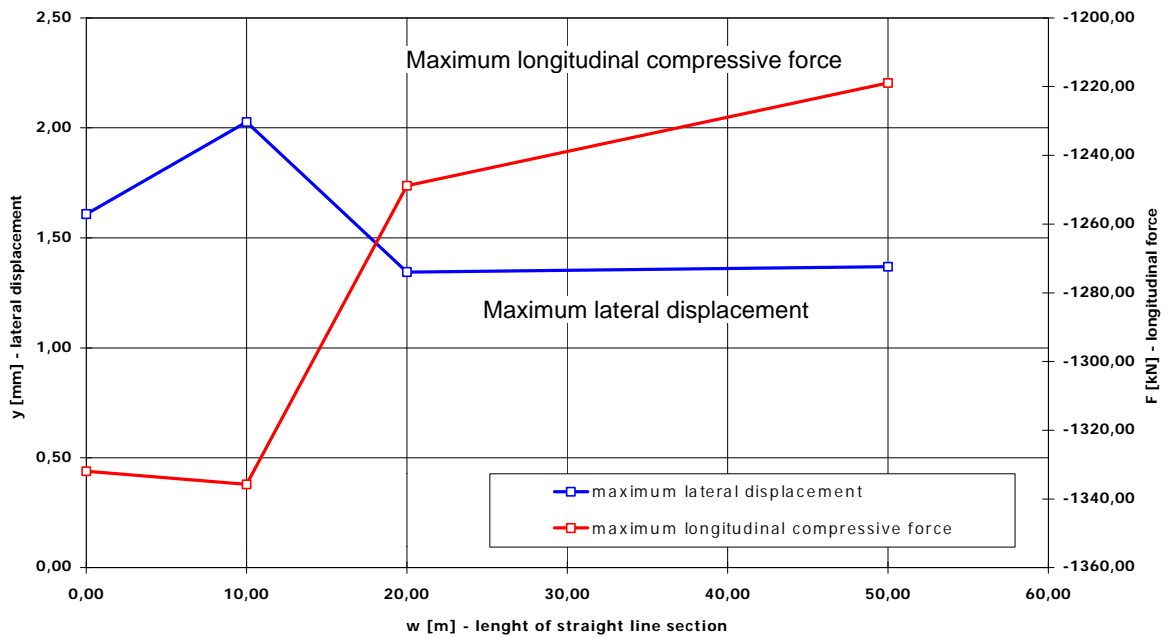


Figure 33 Effect of length of a section "w" on the maximum lateral displacement and maximum longitudinal compressive force in the external rail

### 3.5 Distribution of CWR forces due to tamping

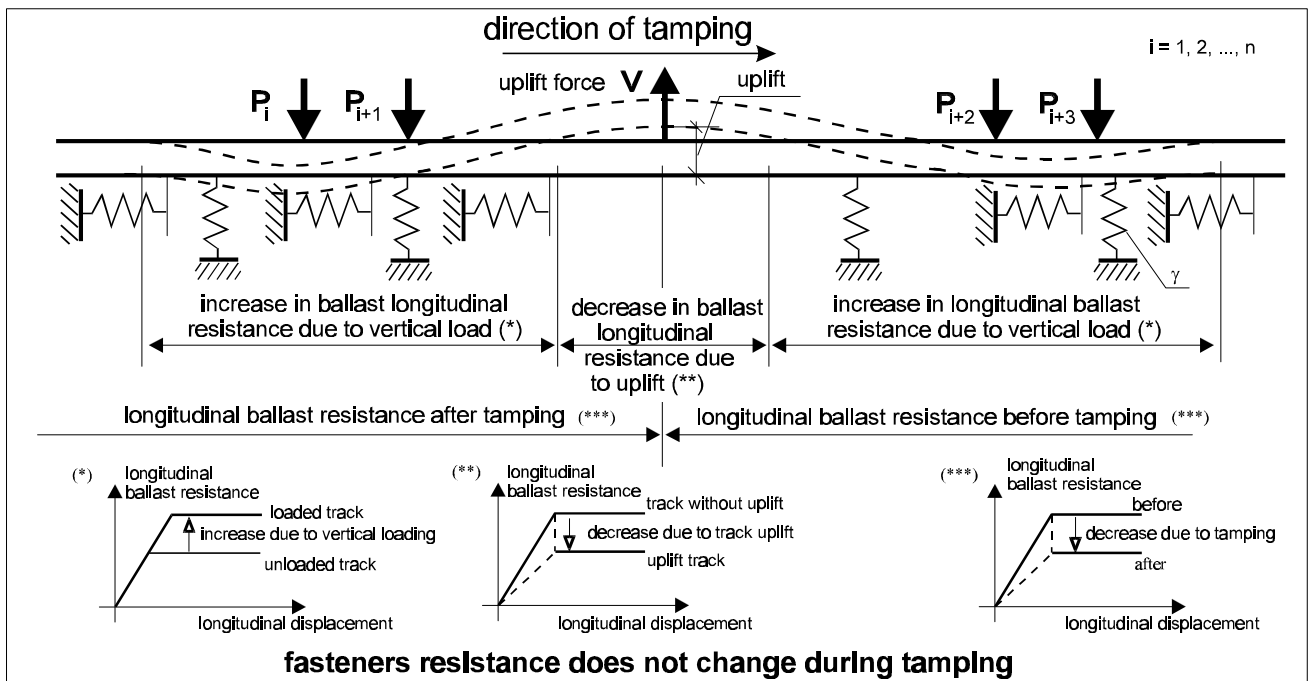


Figure 34: Model of tamper

In the creep analysis with LONGIN the load is considered as a quasi-static moving load. The effect of the change in longitudinal resistance under vertical load is included. Ballast and fastener resistance are modeled bi-linearly, while it is further assumed that the ballast deteriorates with the number of brake applications according to a decaying exponential function.

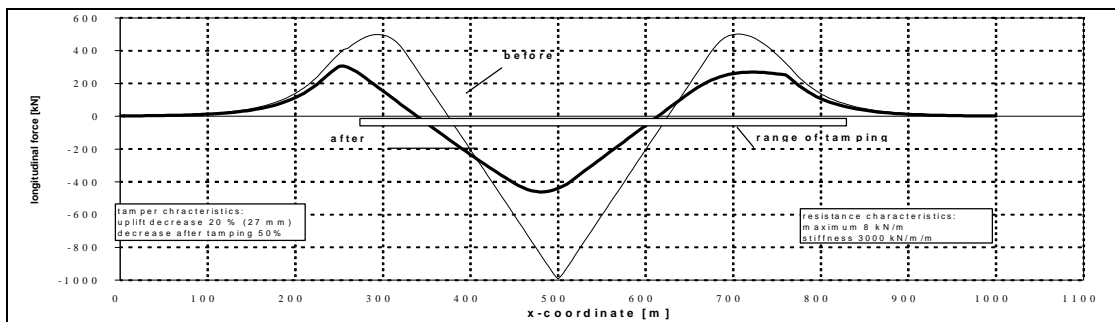


Figure 35: Distribution of residual longitudinal track force before and after tamping

LONGIN also allows analysis of the lateral breathing of curves [5]. A number of cases were computed, to study the breathing behaviour of sharp curves. The results showed how important a role ballast properties play.

The influence of track maintenance (tamping) on the redistribution of longitudinal rail forces is illustrated with a number of calculations. The analyses were made for a track with assumed initial residual longitudinal strain (longitudinal force) and no thermal force. The model of the track machine is shown in Figure 34.

Figure 35 shows distributions of the longitudinal track force before and after tamping. Figure 36 displays the influence of the uplift and the amplitude of the initial residual force on the value of the force remaining in the track after tamping for a chosen half wavelength of 200 m. Figure 37 shows the influence of the loosening of ballast due to tamping on the reduction of the residual force for different half wavelengths of residual (initial) force.

From the calculations it follows that:

- 1) The rate at which the longitudinal force decreases depends mainly on the total reduction in ballast resistance after tamping (that is 25%, 50% or 75%). The amplitude of the initial residual force in the track also influences the rate of the reduction.
- 2) For small amplitudes the rate of reduction is small (nearly 100% of the force remains in the track). For larger force amplitudes the decrease is more significant and varies about the rate by which the ballast resistance decreased after tamping.
- 3) The influence of uplift is less significant and ranges from 10% to 30%, being higher where the half wavelengths of the initial residual force are shorter.

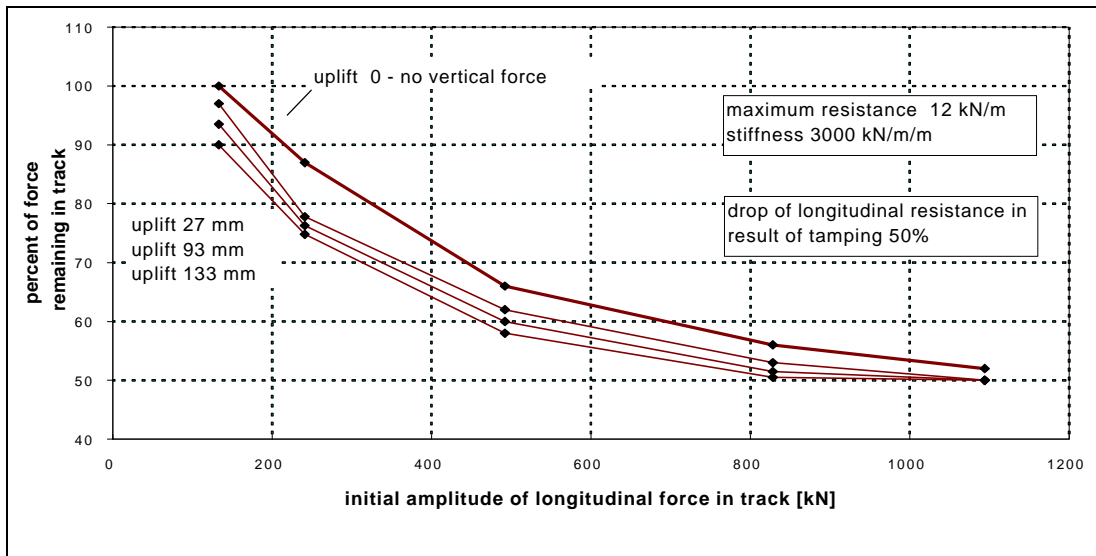


Figure 36: Decrease in the longitudinal rail force after tamping as a function of the initial amplitude of the longitudinal rail force

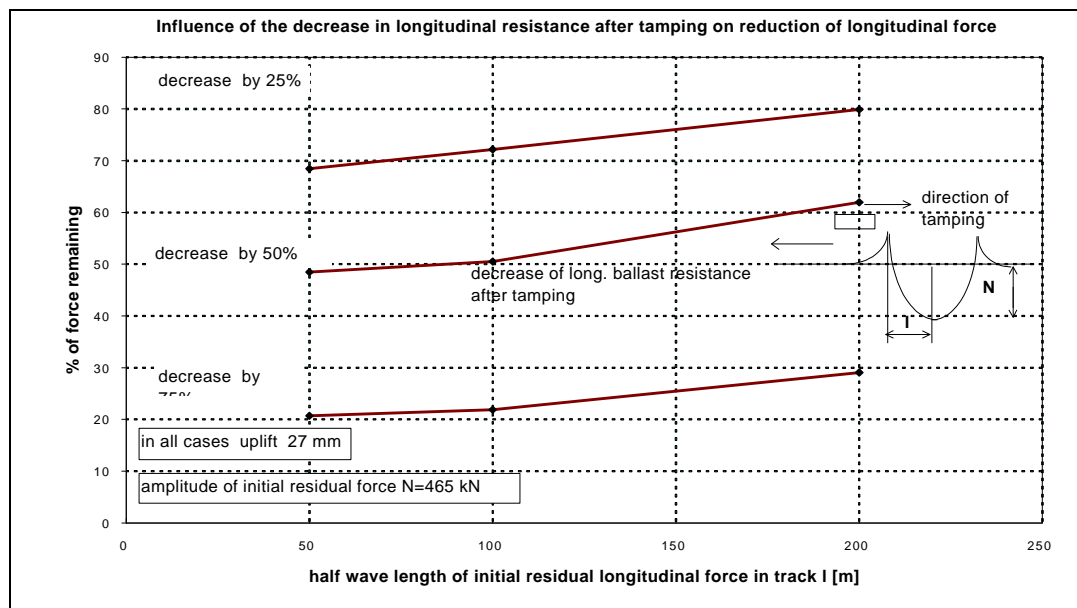


Figure 37: Influence of the decrease in the longitudinal resistance after tamping (loosening of ballast) on the reduction of longitudinal force

## 4. LATERAL/LONGITUDINAL RESISTANCE MEASUREMENTS

An experimental programme was conducted to determine the lateral resistance characteristics to be employed in the models CWERRI, LONGIN and TURN. Tests were carried out as follows:

- Lateral resistance tests in a test track situation carried out by BR Research, and described in detail in Reference [14].
- Lateral resistance tests in a service track carried out by DB, and described in detail in Reference [13].
- Lateral ballast and longitudinal fastening and ballast resistance tests in a laboratory carried out by TU Delft, and described in detail in Reference [15].
- Lateral and longitudinal resistance tests in a service track, as part of the long term longitudinal creep tests performed by MÁV, and described in detail in Reference [16].
- Longitudinal ballast resistance tests in a service track, as part of the long term creep tests performed by PKP/T.U. Krakow, and described in detail in Reference [17].

A synthesis report of the lateral and longitudinal resistance tests was also produced (Reference [7]), which gave details of the recommended parameters to be employed in CWERRI, LONGIN and TURN.

The lateral ballast resistance is considered to have the characteristic shape illustrated in Fig. 38, and the characteristic parameters defining this shape were therefore extracted from the test data. These parameters are also those employed in the ballast resistance definition within CWERRI and LONGIN.

The test programme also covered a range of normal track operating conditions and provided data on the requirements for modelling. The following conditions were investigated:

- Strong, medium and weak ballast conditions were considered for determining the lateral resistance of concrete monoblock sleepers. Strong track had an adequate shoulder of well consolidated ballast, whereas weak track had a shortage of ballast, which was not consolidated. This latter condition was therefore considered to be appropriate for track that has been just maintained. The results obtained from these tests by various administrations were consistent with each other, and with historical data, giving confidence in the results obtained.
- The lateral resistance of twin block sleepers was also determined. In the laboratory tests, the resistance was found to be significantly higher than that measured for monoblock sleepers (by about 60%), but in the track tests conducted by DB the difference was smaller (around 35%).
- The lateral and longitudinal resistance under different vertical loads was investigated (including the case of complete unloading). This enabled the effective coefficient of friction for concrete sleepers to be determined. This parameter is employed in CWERRI when the dynamic case with vehicle loading on the track is considered.
- A limited investigation was made to determine the influence of vertical vibration on lateral resistance, to consider the possible influence of vibration from passing trains. A relatively severe level of vibration was employed, but this did have a significant effect on the maximum lateral resistance. It was considered desirable to pursue this discovery further, but this was not possible within the constraints of the current study.
- The influence of longitudinal and vertical loading on the lateral resistance was determined by means of a laboratory test. This permitted the obtained relationships to be incorporated into CWERRI.
- The rail/sleeper and sleeper/ballast longitudinal resistance values were determined from the laboratory test programme. Longitudinal resistance of the ballast was also determined for some service tracks.

Examples of the lateral resistance test data for typical cases with strong, medium and weak ballast are shown in Figs. 39, 40 and 41.

## 4.1 Conclusions of the Lateral Resistance Testing

The test programme was effective in determining the parameters to be employed in a lateral stability model such as CWERRI or CWRBUCKLE. In order to consider potentially the worst case parameters for the design case, the parameters shown in Table 2 were recommended as starting values for a typical analysis.

	Peak resistance $F_p$ (kN)	Displacement $W_p$ (mm)	Min. resistance $F_l$ (kN)	Displacement $W_l$ (mm)
Loose Tamped/Relay (Weak)	5.2	15	5.2	40
Just Tamped –Undisturbed (Medium)	7.1	10	6.2	40
Trafficked (Strong)	8.1	5	6.7	40

Table 2 Recommended Lateral Resistance Characteristic Values per Sleeper

The coefficient of friction to be employed for lateral ballast resistance on concrete sleepers should be 0.86. This parameter is employed in CWERRI when the dynamic case with vehicle loading on the track is considered.

## 4.2 Conclusions of the Longitudinal Resistance Testing

The typical value of longitudinal resistance for concrete sleepers in ballast was determined to be around 11 kN/sleeper. This maximum value was reached at a deflection of around 5 mm.

For the typical elastic fastening and resilient rail pad tested, the longitudinal resistance was found to be around 19 kN/sleeper (two rails), although the value is known to be influenced by the type of fastening, rail pad and sleeper employed.

The coefficient of friction determined for longitudinal resistance on concrete sleepers with elastic fastenings and resilient rail pads was 0.73 for the sleepers in the ballast, and 0.23 for the rail on the sleeper. Due to the toe load the actual resistance of the rail to the sleeper is higher than of the sleeper to the ballast.

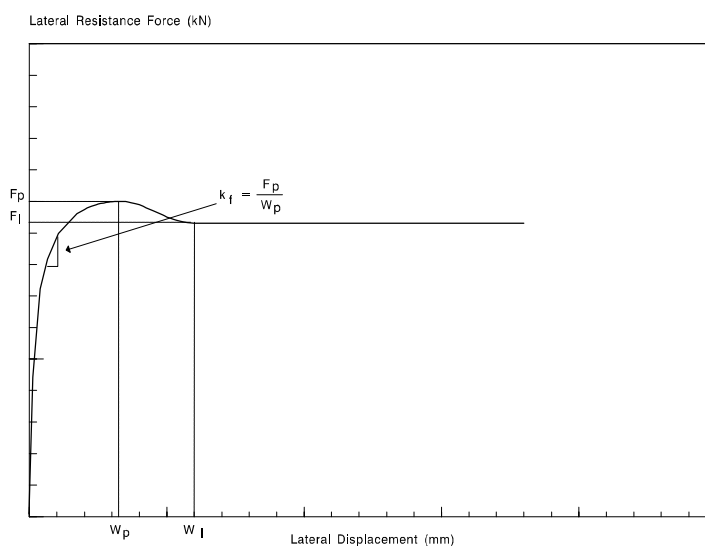


Fig 38 Lateral Resistance Characteristic Values

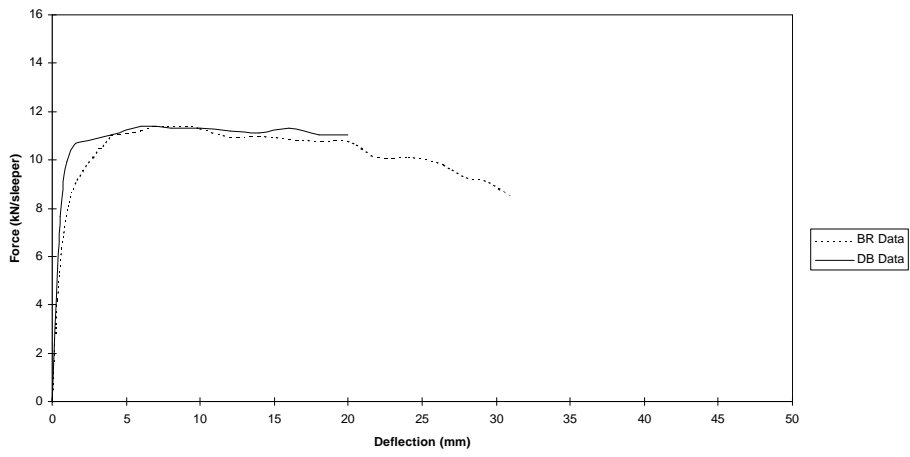


Fig 39 Lateral Resistance Test Data for Strong Track

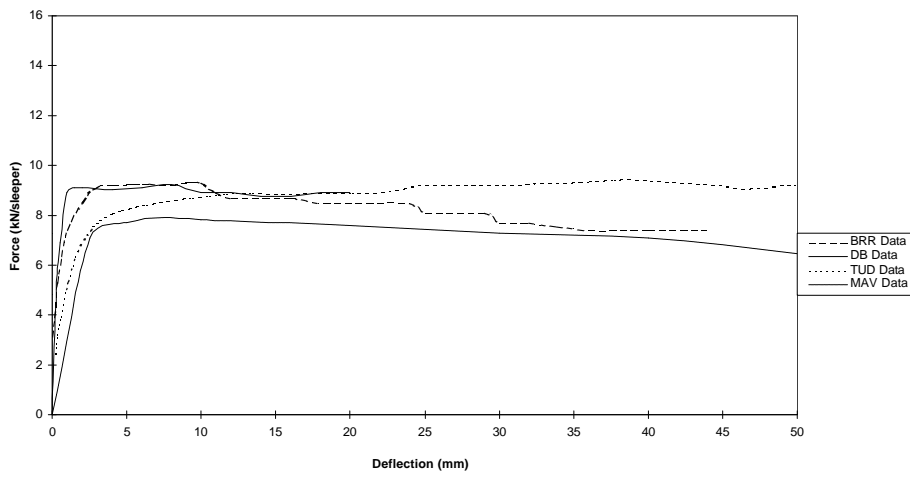


Fig 40 Lateral Resistance Test Data for Medium Track

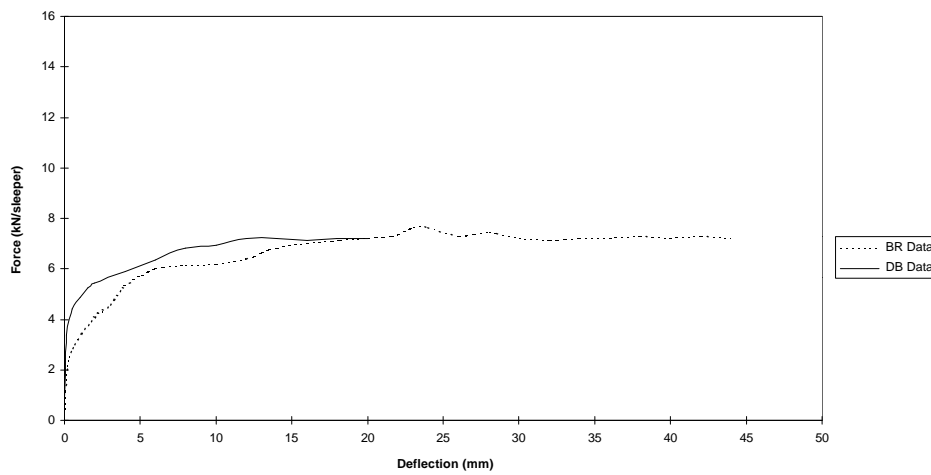


Fig 41 Lateral Resistance Test Data for Weak Track

## 5. LONG TERM BEHAVIOUR

### 5.1 Introduction

Neutral rail temperature may change in time in continuously welded rail tracks. Changes may be expected in places where rail creep may occur in the following conditions:

- train acceleration, braking especially in combination with gradient,
- in sharp curves as an effect of inward/outward movement,
- as a consequence of track maintenance operations, like track tamping, destressing, ballast cleaning, etc.

The empirical investigations which were carried out by PKP, MAV and TU-Kraków in the 1996-1997 years are summarized in [8]. The research concerns changes of longitudinal forces and rail displacements during service in various track and load conditions. The basis of the report are the following documents [16] and [17].

### 5.2 State of art on long-term CWR track behaviour and the aim of the research

Empirical research of CWR track behaviour mainly concern the following problems:

- a) response of buckled track (including full scale tests),
- b) determination of lateral and axial resistance in laboratory and field conditions

Further distinction could be made between publications on turnouts and adjoining track response under one-way (unrepeated) thermal loading and the interaction between the track and a bridge in longitudinal direction. Few papers were published on the long-term effect. The results of the existing work on long term CWR track response may be summarized by the following statements:

1. Changes of NRT (Neutral Rail Temperature) during service may reach  $\pm 10$  °C. General tendency was for the NRT to shift down wards,
2. For typical train loads and track structure the longitudinal residual displacements due to track creep are equal to a few millimeters. In particular cases for very heavy trains longitudinal residual displacements may reach about 500 mm per year,
3. Once thermal loading of turnout and adjoining zones may be characterized as follows:
  - a) longitudinal force in switch rails zone may increase up to 50% in relation to the thermal force for straight track,
  - b) longitudinal displacements in the straight track reaches 2 to 10 mm.
4. Longitudinal track response due to elongation/shortening of bridge deck practically does not depend on service time.

The aim of the research is improvement of knowledge of long-term CWR track response by:

1. Simultaneous day and night measurements of longitudinal and lateral rail displacements, longitudinal forces in rails as well as temperature of rails in the following conditions (straight line sections, sharp curves, turnouts and adjoining zones)
2. Long-term investigation of track response during service.

### 5.3 Characteristics of test track sections

Long-term investigations of CWR track behaviour were designed for the following condition:

- a) straight line sections (6 sections in Poland and 2 sections in Hungary)
- b) sharp curves (6 sections in Poland and 4 sections in Hungary)
- c) interaction between welded turnouts and adjoining zones (3 sections in Poland)

Characteristics of the test track sections may be summarized as follows:

1. Total number of test sections: 21
2. Total length of test sections: about 7 km
3. Length of each sections: 200 to 550 m
4. Curvature: 300 m to straight
5. Gradient of the line: 0 to 21 ‰
6. Measurement period: minimum 9 months
7. Annual load: 4,9 to 41 MGT/year
8. Track structure:
  - a) rails: UIC-60, UIC-54 and S-49
  - b) sleepers: concrete and or wooden
  - c) fastening type: K, Skl, SB-3
  - d) ballast: crushed stone; 0.25 to 0.60 m under sleeper
9. Traffic structure: mixed or only freight trains
10. Train speed:
  - a) passenger: 60 to 140 km/h
  - b) freight: 60 to 70 km/h
11. Special circumstances: level crossings, steel and concrete ballasted bridges and braking zones
12. Maintenance operations during investigation period (on individual sections): destressing, tamping and ballast cleaning

As can be seen track and load conditions are quite variable and cover practically all European situations, excluding high speed and special lines.

#### **5.4 Measurement quantities and equipment**

Long-term CWR track behaviour were investigated by the measurement of the following quantities:

1. longitudinal force in rails:
  - a. relative measurement of rail base elongation /shortening using Pfender device and additionally rail temperature (measurement in Hungary),
  - b. relative measurement of rail base elongation/shortening with automatically inclusion rail temperature using MS-02 device (measurement in Poland),
  - c. typical strain gauge method (measurement in Hungary),
  - d. magneto-elastic absolute (not relative) measurement methods using RAILTEST and RAILSCAN equipment (measurement in Hungary),
2. longitudinal and lateral rail displacements:
  - a. measurement in relation to the fixed points - using MP-device (in Poland)
  - b. measurement in relation to the fixed points - using geodetic methods (in Hungary)
3. rail temperature,
4. track and ballast resistance using special Polish and Hungarian devices.

Also control measurement of track state by EM-120 measuring car (in Hungary) and by use of the typical geodetic method (in Poland).

Comparative measurement of longitudinal force using Polish and Hungarian equipment were carried out on both test track sections.

Knowing the value of longitudinal force  $N_L$  [kN] and actual rail temperature  $T_a$  [°C] the neutral rail temperature (NRT) is calculated according to the formula:

$$NRT = \frac{N_L}{\alpha EA_r} + T_a \quad [^{\circ}\text{C}]$$

where:

$\alpha$  - coefficient of thermal expansion for rail steel [1/°C],

$E$  - Young modulus [kN/m<sup>2</sup>],

$A_r$  - cross-section of rail [m<sup>2</sup>]

The accuracy of the measurement quantities may be estimated on the following levels:

- a) neutral rail temperature (NRT)  $\pm 3$  °C
- b) longitudinal and lateral displacements  $\pm 0.1$  to 0.5 mm depends on the applied method.

## 5.5 Results of the measurements and their analysis

The measurements were carried out as:

- a. short-term response (day and night investigation of changes of longitudinal forces and rails displacement) including actual rail temperature,
- b. long-term effects - changes of NRT during service, estimation of trends of changes of rail displacements, etc.

Fig.42 shows a typical short-term track response on the straight section (S3). At the same time the lateral movements reach a few millimeters.

Fig 43 and 44 present changes of average NRT for selected test track sections. The results of geodetic and fixed points measurements proved that, as expected, there were changes of a few millimeters in the direction of the radius in the curves under the effect of low winter and high summer temperatures.

Longitudinal rail displacement also reached a few mm and in certain cases it was as big as 10 mm. From the presented results and additional analyses the following conclusions could be formulated:

1. Changes in NRT during service reached 5 to 20 °C (see Fig. 7.1-7.6)
2. Changes of NRT during service had, in general, a form of a random variation without distinct trend.
3. CWR track with concrete sleepers gave more stable NRT during service in relation to the track with wooden sleepers.
4. The average NRT values calculated for the test sections were not constant in the curves but shown the annual periodicity of the rail temperature.
5. Lateral displacements in the switch zone of welded turnouts may reach  $\pm 2$  to 3 mm. It means that special protection (in particular for turnouts with wooden sleepers) must be introduced for limitation of displacement only to the elastic response.
6. Use of devices with NRT measurement accuracy at the level of  $\pm 3$  °C and displacement measurement accuracy of about 0.1 to 0.2 mm are practically sufficient for investigation of CWR track behaviour without considering special local effects (e.g. distribution of residual stresses in rail cross-section, local changes of rail material microstructure etc.). To measure the actual NRT of a given section before major track maintenance operations to enable the most suitable technology to be chosen.

## 5.6 Summary and general conclusions

Long-term investigations of CWR track behaviour were carried out for various track and load conditions, excluding high speed and special lines. The investigations improved the knowledge of CWR behaviour and may be useful for validation of theoretical models. Certain practical conclusions, stated in the previous section, might be applied by railway companies. Further investigations could be oriented on the following topics:

- investigation of the effect of heavy train braking on the track response, especially with respect to the measure of dynamic braking longitudinal forces and dynamic/residual force and displacements in rails,
- improvement of knowledge of rheological track properties, especially with respect to the ballast behaviour,
- improvement of measurement equipment from the point of view of their accuracy and durability,
- further investigation of sharp curve behaviour and long-term response of welded turnouts,
- further investigation of ballasted and ballast less track on bridges, especially with respect to the interaction between track and bridge in longitudinal as well as vertical directions.

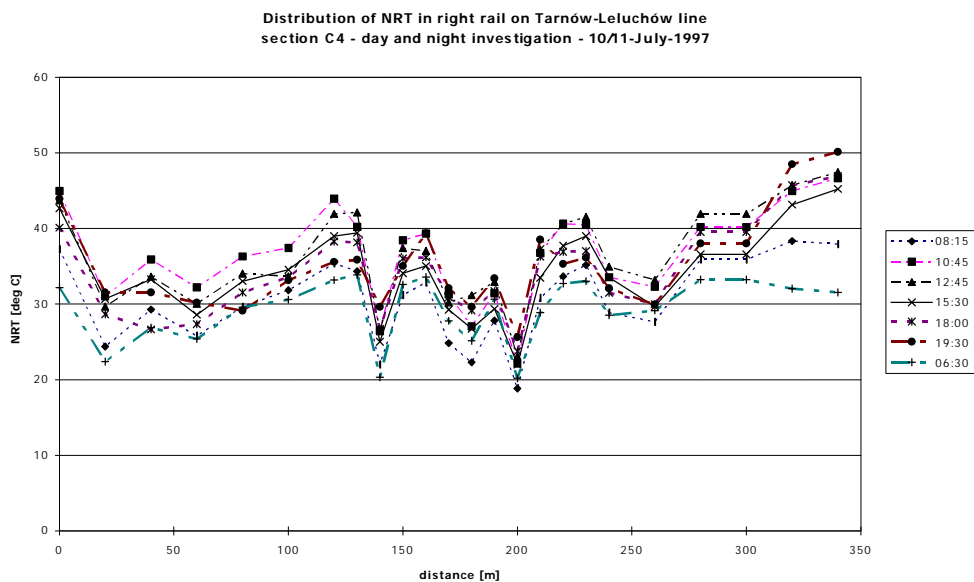


Fig. 42 Short-term track response

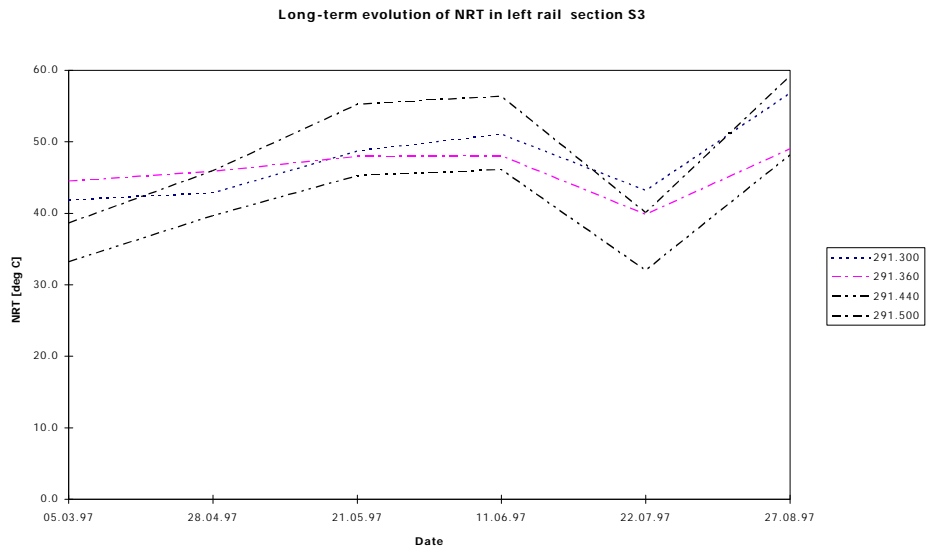


Fig. 43 Changes of NRT

Note: differences between the NRT values in June, July and August are caused by large air temperature variations in summer season

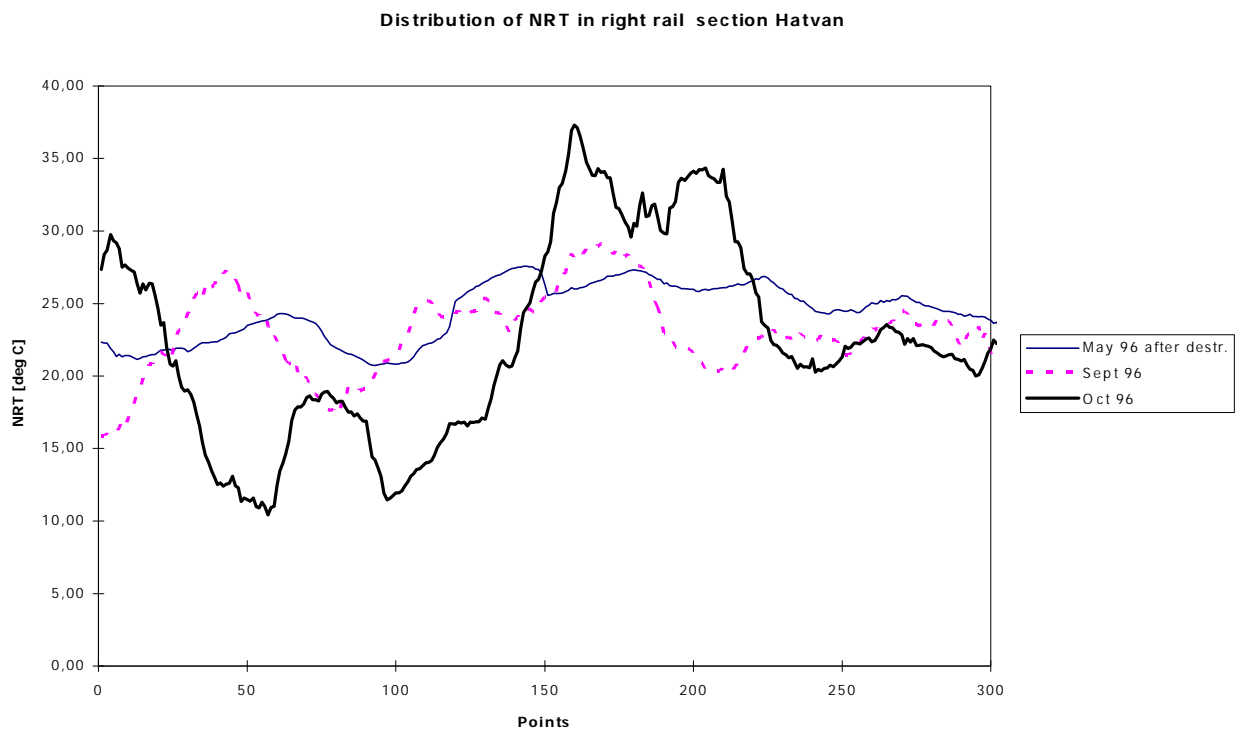


Fig. 44 Changes of NRT

NRT changes along the section C.10 measured with RailScan within five months after distressing

## 6. NON-DESTRUCTIVE MEASUREMENT OF CWR FORCES

### 6.1 Introduction

The question of the non-destructive measurement of longitudinal forces was tackled as part of the work of the D 202 Committee "Improved knowledge of forces in CWR track (including switches)" of the European Rail Research Institute (ERRI), and further investigations were carried out in connection with the most promising systems:

- ◆ the DB ultrasonic method,
- ◆ the DB method for strain and length measurements
- ◆ the MAV Barkhausen method (magneto-elastic method),
- ◆ the MAV strain gauge method, and
- ◆ the MAV Pfender measuring method.

Although various methods exist to measure absolute stresses, it is very complicated to determine absolute rail forces accurately. This is due to the extremely high residual stresses introduced during the roller straightening process to meet the tight straightness tolerances of rail geometry. Figure 45 shows the distribution of residual stresses in new rails (as-rolled) and in used rails as measured by ORE D 148.

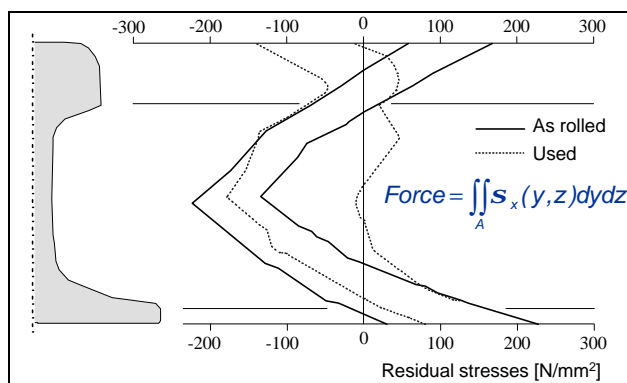


Figure 45 Residual stresses measured by ORE D 148

### 6.2 Summary of the work at Fraunhofer Institute

Ultrasonic techniques to evaluate stress states are based on the acousto-elastic effect. The ultrasonic velocities or times-of-flight are influenced by the strain or stress state of the material. The proportionality between stresses and times-of-flight is described in terms of the acousto-elastic constants. The acousto-elastic constants of rails manufactured by three different plants have been evaluated together with their temperature dependency. The acousto-elastic constants are found to be different for samples cut from the rail head and from the rail web; the individual manufacturer has not an influence on the inspection results. Because of the temperature dependency, two sets of elastic constants covering the application in a low temperature and in an elevated temperature range are determined.

Beside of stress, also texture influences the direction dependence of ultrasonic velocities. The texture in new and used rails and its influence on the measuring quantities have been measured. Different texture grades are found in the head and in the web area of rails. The influence of texture on the shear waves propagating the total height of the rails is found to be small. The texture is homogenous along the inspected parts of the rail lengths.

The stress state in new and used rails was evaluated using the well-established ring core technique. Measurements were made on the running surface, on the outer side of the head, as well as on the flange. The change of the stress state was taken as function of the depth up to 5 mm of depth. The assumption of a one axial stress state with the dominant stress in the length direction is justified only for new rails. In used rails, the significant contributions of the stresses in the width direction onto the velocities of ultrasonic waves have to be taken into account. Based on these

results, it is concluded to use different techniques in order to evaluate the stress states in new and in used rails.

The state of the art of the ultrasonic techniques to evaluate stress states in components is most recently described in *Structural and Residual Stress Analysis by Nondestructive Methods*, edited by Viktor Hauk, published by Elsevier Amsterdam in 1997. In order to evaluate the stress states of rails in the track, the concept of applying two ultrasonic shear wave modes is seen as the most promising way using ultrasonic techniques.

Recent improvements of the electromagnetic techniques, as described in the above mentioned book, offer a nondestructive technique which might be even more suitable than the ultrasonic techniques. With one sensor different electromagnetic and magneto-elastic quantities are measured. A multi-parametric regression algorithm is applied to evaluate the stress state and the hardness value. At present, the technique and the set-up are tested using the rails, already inspected with the ultrasonic techniques.

### **6.3 SUMMARY AND NEED FOR RESEARCH**

The DB ultrasonic method and the MAV Barkhausen method showed themselves to be the most promising. Both methods can be used not only under laboratory conditions but also in normal practice. The DB research work needs to be completed during the remaining development period. MÁV are quite prepared to make use of their method in practice on their own network. It would therefore be advantageous to arrange for both methods to be tested on other railways as well under different operating and climatic conditions, if only to get the opinion of independent specialists about the practical use of the recommended methods.

## **7. DELIVERABLES**

### **7.1 Reports**

The Committee's deliverables are consisting primarily of reports and computer programs. There are 12 reports describing the theoretical and experimental work, the development of computer programs and the use of those computing tools. The reports are referred to as references [1] to [12].

Additionally six Technical Documents (DTs) were published (see references [13] to [18]), describing the details of experiments and special studies

### **7.2 Programs**

The following programs were delivered:

1. CWERRI : General purpose program for the analysis of continuous welded rail track;
2. LONGIN: Analysis of general creep problems;
3. TURN: Analysis of turnouts in combination with the finite element package ALGOR. The program ALGOR is not a deliverable to ERRI. ERRI should further consider how to deal with licenses.

Furthermore, the general track buckling analyses program CWR-Buckle was made available to the D 202 Committee by Volpe/DOT.

## **8. CONCLUSIONS**

From the work of the D 202 Committee the following conclusions could be drawn:

1. The theory of track buckling has been developed by D 202 to such a stage that the major influences of physical and geometrical non-linearities, as well as some dynamic influences, have been implemented in computer models;
2. With CWERRI track behaviour in longitudinal direction can be described and the resulting force distribution can be used as the basis for a buckling and safety analysis;
3. A safety philosophy was developed by the D 202 Committee and this was implemented in the draft of UIC Leaflet 720 presented in RP 10. The programs developed by D 202 are essential tools to be used in combination with the new leaflet;
4. With the program LONGIN a general purpose creep analysis tools was developed for analyzing long-term movements in the track and the effects of track maintenance form the point of redistribution of forces;
5. A tool has been developed for the analysis and design of long-welded turnouts and sharp curves; the calculations are performed in combination with the FEM-package ALGOR, which is not a deliverable;
6. With the tests carried out by D 202 valuable information on lateral resistance data, longitudinal resistance data and creep data was obtained; the creep behaviour laws could be verified and input data for the programs CWERRI, LONGIN, TURN and CWR-Buckle could be collected.

## **9. RECOMMENDATIONS**

The D 202 Committee came to the following recommendations:

1. Although the theory on track stability has been developed to quite a high standard, further work is needed on modeling of vehicle induced buckling;
2. The development of track geometry imperfections, due to successive passes of vehicles, could eventually lead to track buckling. It is advised to continue studying and modeling this ratcheting phenomenon;
3. In the time scale available the D 202 Committee was not successful in advising improved methods with regard to non-destructive measurement of CWR forces. As there is a large demand from the railways to come with reliable measuring methods it is strongly advised to pursue research on this subject.
4. The influence of vibrations appeared to have a substantial influence on lateral resistance. It is recommended to further investigate this phenomenon.

## 10. REFERENCES

- [1] ERRI D202/RP1: 'Proposal for theoretical model investigations concerning CWR', August 1994.
- [2] ERRI D202/RP2: 'Review of existing experimental work on behaviour of CWR track', February 1995.
- [3] ERRI D202/RP3: 'Theory of CWR track stability', February 1995
- [4] ERRI D202/RP4: 'Stability of continuous welded rail track', June 1997
- [5] ERRI D202/RP5: 'Analysis of factors that influence the longitudinal behaviour of CWR track including lateral movement of sharp curves', November 1997
- [6] ERRI D202/RP6: 'Analyses of turnouts', November 1997
- [7] ERRI D202/RP7: 'Sleeper Lateral resistance Measurements: Synthesis Report', December 1997
- [8] ERRI D202/RP8: 'Long term creep tests', December 1997
- [9] ERRI D202/RP9: 'Non-destructive force measurements', December 1997
- [10] ERRI D202/RP10: 'Draft UIC 720', November 1997
- [11] ERRI D202/RP11: 'Parametric study and sensitivity analysis of CWERRI', October 1997
- [12] ERRI D202/RP12: 'Final report', December 1997
- [13] ERRI DT 360: Reinicke, Herrmann and Parmentier ERRI D202 / WG 3 Lateral Resistance Tests REPORT 50548, DB, October 1997.
- [14] ERRI DT 361: Hunt, G.A. and Yu, Z.M. Measurement of Lateral Resistance Characteristics for Ballasted Track BR Research Report RR-TCE-81, January 1997.
- [15] ERRI DT 362: van 't Zand, J. and Moraal, J. Ballast Resistance under Three Dimensional Loading DRAFT REPORT 7-96-103-4, TU Delft, December 1996.
- [16] ERRI DT 363: Vol. I: Rail Creep due to Traction/Braking, Change of NRT due to the movements of sharp curves; Vol. II Determination of Lateral and Longitudinal Ballast Resistance of a Railway Track by Experimental Tests, MÁV October 1997.
- [17] ERRI DT 364: Czyczula, W. Empirical research of CWR long term behaviour for ERRI D202/3, November 1997
- [18] ERRI DT 365: Kish, A., G. Samavedam and J. Gomes: 'CWR-BUCKLE User's Guide' US Department of Transportation.
- [19] Van, M.A. : 'Stability of Continuous welded Rail Track', Delft University Press, Dissertation TU Delft, June 1997
- [20] Samavedam, G., A. Kish, A. Purple and J. Schoengart: 'Parametric Analysis and Safety Concepts of CWR Buckling', US DOT-VNTSC-FRA-93-25, December 1993